THE JOURNAL OF BIOLOGICAL CHEMISTRY VOL. 283, NO. 17, pp. 11501–11508, April 25, 2008

Adaptor Protein Sorting Nexin 17 Regulates Amyloid Precursor Protein Trafficking and Processing in the Early Endosomes*

Received for publication, January 24, 2008, and in revised form, February 13, 2008 Published, JBC Papers in Press, February 13, 2008, DOI 10.1074/jbc.M800642200

Jiyeon Lee[‡1], Claudio Retamal[§], Loreto Cuitiño[§], Amy Caruano-Yzermans[‡2], Jung-Eun Shin[‡], Peter van Kerkhof[¶], Maria-Paz Marzolo[§], and Guojun Bu[‡3]

From the [‡]Departments of Pediatrics and Cell Biology and Physiology, Washington University School of Medicine, St. Louis, Missouri 63110, the [§]Centro de Regulación Celular y Patología "Joaquín V. Luco," Departamento de Biología Celular y Molecular, Millennium Institute For Fundamental and Applied Biology, Facultad de Ciencias Biológicas, Pontificia Universidad Católica de Chile, Santiago 340, Chile, and the [¶]Department of Cell Biology and Institute of Biomembranes, University Medical Center, Utrecht 3584 CX, The Netherlands

Accumulation of extracellular amyloid β peptide (Aβ), generated from amyloid precursor protein (APP) processing by β- and γ-secretases, is toxic to neurons and is central to the pathogenesis of Alzheimer disease. Production of Aβ from APP is greatly affected by the subcellular localization and trafficking of APP. Here we have identified a novel intracellular adaptor protein, sorting nexin 17 (SNX17), that binds specifically to the APP cytoplasmic domain via the *YX*NP*XY* motif that has been shown previously to bind several cell surface adaptors, including Fe65 and X11. Overexpression of a dominant-negative mutant of SNX17 and RNA interference knockdown of endogenous SNX17 expression both reduced steady-state levels of APP with a concomitant increase in Aβ production. RNA interference knockdown of SNX17 also decreased APP half-life, which led to the decreased steady-state levels of APP. Immunofluorescence staining confirmed a colocalization of SNX17 and APP in the early endosomes. We also showed that a cell surface adaptor protein, Dab2, binds to the same *YX*NP*XY* motif and regulates APP endocytosis at the cell surface. Our results thus provide strong evidence that both cell surface and intracellular adaptor proteins regulate APP endocytic trafficking and processing to Aβ. The identification of SNX17 as a novel APP intracellular adaptor protein highly expressed in neurons should facilitate the understanding of the relationship between APP intracellular trafficking and processing to Aβ.

Mounting evidence has demonstrated that proteolytic processing of the amyloid precursor protein (APP)[4] is central to the pathogenesis of Alzheimer disease (AD) (1, 2). Many reports have shown that APP processing to Aβ is greatly affected by the subcellular localization of APP, presumably because of the specific subcellular localizations of β- and γ-secretases (3). Both transmembrane receptors and cytoplasmic adaptor proteins have been shown to interact with APP and affect its trafficking. The low-density lipoprotein receptor-related protein 1 (LRP1) increases APP endocytosis and Aβ production (4), whereas SorLA decreases APP processing to Aβ by shuttling APP away from endosomes (5). Several cell surface adaptor proteins, including Fe65, X11, and Dab1, bind to the NP*XY* motif within the APP cytoplasmic domain and regulate its trafficking and processing to Aβ (6–8). By overexpression or knockdown, Fe65 has been shown to affect APP processing to Aβ (9, 10). Although Dab1 has been shown to affect APP processing and Aβ production (11), the function of its homologue Dab2 in APP trafficking and processing to Aβ has not been studied (8). These studies firmly establish that APP-interacting proteins can both positively and negatively affect Aβ production by altering APP trafficking through β- and γ-secretase-containing compartments. Revealing the mechanisms by which intracellular trafficking of APP is regulated may permit the development of novel therapeutic approaches for AD.

Sorting nexin 17 (SNX17) is a member of the sorting nexin family characterized by the presence of a phox (PX) domain (12), which serves to localize SNX17 to intracellular vesicles by interacting with specific phosphatidylinositol phosphates (13, 14). Like many sorting nexins, SNX17 is localized to early endosomes (15–17). SNX17 has been shown to interact with several LDLR family members, including LDLR and LRP1, through the NP*XY* motifs in their cytoplasmic domains (15–17) and to regulate their endocytic trafficking. In this study, we demonstrate that SNX17 serves as an intracellular adaptor protein for APP

* This work was supported in part by NIA Grant R01 AG027924 from the National Institutes of Health, a grant from the Alzheimer's Association, and a grant from the American Health Assistant Foundation (to G. B.). This work was also supported by Fogarty International Research Collaboration Award Grant TW006456 (to G. B. and M.-P. M.), Fondo de Investigación Avanzada en Areas Prioritarias Grant 13980001, and a grant from the Millenniums Institute for Fundamental and Applied Biology (to M.-P. M.). The costs of publication of this article were defrayed in part by the payment of page charges. This article must therefore be hereby marked "*advertisement*" in accordance with 18 U.S.C. Section 1734 solely to indicate this fact.

[1] Partially supported by a predoctoral fellowship from the American Heart Association.

[2] Present address: Divergence Inc., 893 North Warson Rd., St. Louis, MO 63141.

[3] To whom correspondence should be addressed: Dept. of Pediatrics, WA University School of Medicine, Campus Box 8208, 660 South Euclid Ave., St. Louis, MO 63110. E-mail: bu@wustl.edu.

[4] The abbreviations used are: APP, amyloid precursor protein; Aβ, amyloid β peptide; ELISA, enzyme-linked immunosorbent assay; AD, Alzheimer disease; LRP, low-density lipoprotein receptor-related protein; HA, hemagglutinin; siRNA, small interfering RNA; GST, glutathione *S*-transferase; PTB, phosphotyrosine-binding domain; PBS, phosphate-buffered saline; CHO, Chinese hamster ovary; PX, phox; LDLR, low-density lipoprotein receptor.

and regulates its trafficking and processing to Aβ. We further show that Dab2 mediates APP endocytosis. Our study provides strong evidence that multiple steps of APP endocytic trafficking are regulated by distinct adaptor proteins. The identification of SNX17 as a novel adaptor protein for APP should allow for a new understanding of the cellular mechanisms underlying APP trafficking and processing to Aβ.

EXPERIMENTAL PROCEDURES

Antibodies and Reagents—The polyclonal anti-SNX17 antibody was raised against a 14-amino acid peptide corresponding to the carboxyl-terminal region of SNX17 protein. Polyclonal rabbit anti-SNX17 IgG was purified using protein A beads and used for Western blotting and immunofluorescence experiments. The polyclonal antibody recognizing C-terminal regions of the human and mouse APPs and the monoclonal antibody (6E10) recognizing amino acids 1–17 of Aβ were purchased from Invitrogen and Covance (Berkeley, CA), respectively. Anti-Myc antibody 9E10 was obtained from Sigma. A previously described monoclonal anti-hemagglutinin (HA) antibody was used for Western blot and immunofluorescence staining of APP (18). Fluorescein isothiocyanate-conjugated goat anti-mouse IgG was obtained from BD Biosciences. For enzyme-linked immunosorbent assays (ELISAs), antibodies 21F12, 2G3, and biotinylated 3D6 were the kind gifts of Kelly Bales (Lilly). Carrier-free $Na^{125}I$ was purchased from PerkinElmer Life Sciences. Antibodies were iodinated using the IODO-GEN method as described previously (18).

Plasmids and Fusion Proteins—Mouse SNX17 cDNA tagged at the 5′ end with a 9-Myc epitope and cloned into pCIneo was kindly provided by Dr. Johannes Nimpf (University of Vienna, Austria; see Ref. 16). For an siRNA-resistant Myc-SNX17 construct, eight silent nucleotide mutations were introduced into the sequence targeted by the SNX17 siRNAs. The GST-fused APP cytoplasmic tail construct was generously provided by Dr. Thomas Südhof (University of Texas, Southwestern Medical Center). Constructs of full-length Dab2, the phosphotyrosine-binding domain (PTB) of Dab2, GST-full-length Dab2, and the GST-PTB domain were kindly provided by Dr. Linton Traub (Department of Cell Biology and Physiology, University of Pittsburgh School of Medicine, Pittsburgh, PA). Mutations in the APP tail were introduced by site-directed mutagenesis using the QuikChange mutagenesis kit (Stratagene). All constructs were verified by sequencing. GST fusion proteins were produced in the *Escherichia coli* BL21 strain (Novagen, San Diego, CA) and purified as described previously (19).

GST Pulldown Assay—GST fusion proteins were expressed in bacteria (20), and glutathione beads were added to bind to fusion proteins. Following incubation overnight at 4 °C, beads were washed twice with PBS and resuspended in the same buffer. The U87 stable cell line expressing Myc-SNX17 plasmids or CHO LRP-null cells expressing wild-type or mutant APP were lysed in lysis buffer (20 mM Tris-HCl, pH 8.0, 100 mM NaCl, 1 mM EDTA, 0.5% Nonidet P-40, 1 mM phenylmethylsulfonyl fluoride, and 1× Complete protease inhibitor mixture). Cell lysates were incubated with fusion protein bound to glutathione beads in lysis buffer for 2 h at 4 °C. After washing, beads were boiled in SDS sample buffer and subjected to Western blotting.

Cell Culture and Transfection—Human glioblastoma U87 cells were maintained in Dulbecco's modified Eagle's medium containing 10% fetal bovine serum, L-glutamine, and sodium pyruvate (19). CHO LRP-null cells were grown in Ham's F-12 medium with 10% fetal bovine serum and L-glutamine. U87 cells and CHO LRP-null cells were transfected with various plasmid DNAs using Lipofectamine 2000 (Invitrogen) or TransIT-CHO (Mirus Bioscience, Madison, WI) reagent, respectively.

Western Blot Analysis—Proteins were separated on SDS-polyacrylamide gels under reducing conditions and transferred to an Immobilon-P membrane (Millipore, Billerica, MA). Membranes were blocked in PBS containing 0.05% Tween 20 and 5% nonfat dried milk and subjected to incubation with primary and secondary antibodies. For quantification, blots were developed with ECL Plus reagent (Amersham Biosciences) and were analyzed using a Typhoon 9410 PhosphorImager (Amersham Biosciences).

Aβ ELISA—Cells in 6-well plates were transfected with the constructs to be examined. The next day, the cells were washed twice with low-serum medium (containing 1% fetal bovine serum) and retransfected with the same set of constructs in low-serum medium. Media were collected after 48 h of conditioning and then centrifuged to remove cell debris. Aβ in the media was analyzed by ELISA adapted from previous studies (21). Specially, Aβ in the low-serum medium was captured with antibody 2G3 or 21F12 for Aβ40 and Aβ42, respectively, and was subsequently detected with biotinylated 3D6 antibody. Aβ levels were normalized to the amount of total protein in cell lysates.

SNX17 Knockdown—SNX17 expression was suppressed by transiently transfecting siRNA oligonucleotides as described (17). SNX17 expression was analyzed by Western blotting using anti-SNX17 antibody. Rescue construct for SNX17 was cotransfected into cells with siRNA oligonucleotides, and its resistance to siRNA oligonucleotide against SNX17 was examined by Western blotting using anti-Myc antibody.

Flow Cytometry—For cell surface APP analysis, cells were first detached by incubation with non-enzymatic cell dissociation solution (Sigma). Successive incubations with anti-APP (50 μg/ml) for APP and fluorescein isothiocyanate-conjugated goat anti-mouse Ig were carried out at 4 °C for 1 h. As a control, background fluorescence intensity was assessed in the absence of primary antibody. All measurements were performed on a FACSCalibur (BD Biosciences) equipped with an argon ion laser. Laser excitation of 488 nm for fluorescein isothiocyanate was used. Ten thousand cells from each sample were analyzed. Histograms were generated using the CellQuest software; mean values after subtraction of controls were compared among samples.

Determination of Protein Half-life—Cells were incubated with cycloheximide (100 μg/ml; Sigma) to inhibit further protein synthesis. Following incubation for 0, 15, 30, 45, or 60 min, cells were lysed and subjected to Western blotting. Equal amounts of total protein from each sample were loaded in each lane.

Metabolic Pulse-Chase Labeling and Immunoprecipitation—Metabolic pulse-chase labeling of HA-APP with [^{35}S]Met/Cys was performed as described previously (22). Briefly, cells transiently transfected with HA-APP and control or siRNA oligonucleotide against SNX17 were incubated with medium containing [^{35}S]Met/Cys for 30 min, followed by chasing in medium without [^{35}S]Met/Cys for 0, 0.5, 1, and 2 h. After each time point, cell lysates were incubated with an excess of anti-HA IgG, followed by recovery of the immune complexes with protein A-agarose beads. Immunoprecipitated protein was released from the beads by boiling in Laemmli sample buffer under reducing conditions and analyzed by SDS-PAGE. Radioactive proteins were visualized using a STORM 820 PhosphorImager.

Antibody Uptake and Immunofluorescence Staining—Cells were incubated with anti-HA IgG for 1 h at 37 °C and fixed with 4% paraformaldehyde in phosphate buffer for 20 min at room temperature. After blocking with blocking buffer (PBS containing 0.5% bovine serum albumin), cells were permeabilized with PBS containing 0.2% Triton X-100 and then stained for SNX17 or EEA1, followed by incubation for 1 h with Alexa Fluor 586-conjugated goat anti-mouse IgG to detect mouse anti-HA IgG and anti-EEA1 or Alexa Fluor 488-conjugated goat anti-rabbit IgG to detect rabbit anti-HA IgG and anti-SNX17 antibodies (Molecular Probes, Carlsbad, CA). Cells were mounted in a Cytoseal 60 (Richard-Allan Scientific, Kalamazoo, MI). Cultured rat hippocampal neurons, isolated from day 18 embryos, were fixed in PBS containing 4% paraformaldehyde and 4% sucrose for 20 min. Neurons were permeabilized in PBS containing 0.2% Triton X-100 and incubated with anti-APP (6E10) and anti-SNX17 in PBS containing 0.2% gelatin for 30 min at 37 °C, followed by incubation with Alexa Fluor-conjugated secondary antibody. Stained cells were viewed with a confocal laser scanning microscope (Fluoview 500, Olympus) using a ×60 objective oil immersion lens.

Kinetic Analysis of Endocytosis—Kinetic analysis of receptor-mediated endocytosis was carried out as described previously (18). Briefly, 8 h after cells were transiently transfected in a 6-well plate, cells were replated in a 12-well plate and used after overnight culture. Cells were rinsed twice with cold PBS and then incubated in 0.5 ml of ice-cold ligand binding buffer (Dulbecco's modified Eagle's medium containing 0.6% bovine serum albumin) containing 1 nM ^{125}I-anti-HA IgG for 1 h. After binding, prewarmed binding buffer was added to the cells, and plates were placed in a 37 °C water bath to initiate internalization. After 15 min, the plates were placed on ice, and the ligand binding buffer was replaced with ice-cold stop/strip solution (PBS, pH 2.0). For the 0-min time point, cells were placed on ice immediately after ligand binding and processed as follows. Ligand that remained on the cell surface was stripped by incubation of cell monolayers twice with ice-cold stop/strip solution for a total of 10 min and counted. Cell monolayers were then solubilized with low-SDS lysis buffer (6.25 mM Tris, pH 6.8, 0.2% SDS, 10% glycerol, and bromphenol blue) to release internalized radioactivity. The sum of the internalized ligand plus those on the surface after each assay was used as the maximum potential internalization. The fraction of internalized ligand at each time point was calculated and plotted.

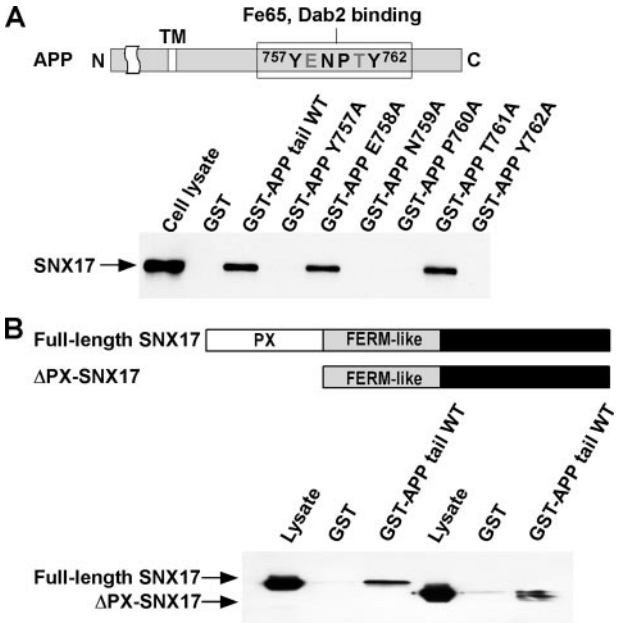

FIGURE 1. **Sorting nexin 17 binds to the APP cytoplasmic domain through the YXNPXY motif.** *A*, a schematic diagram of the APP cytoplasmic domain and GST pulldown assay. GST or GST-APP fusion proteins were incubated with lysates from U87 cells stably expressing full-length SNX17 and subjected to Western blotting with anti-Myc antibody. GST fused with the wild-type (*WT*) APP cytoplasmic domain but not YXNPXY mutants interact with SNX17. *B*, a schematic diagram depicting full-length and PX domain-deleted (ΔPX-SNX17) SNX17 and GST pulldown assay. SNX17 contains a PX domain at the N terminus, a FERM (protein 4.1, ezrin, radixin, and moesin)-like domain, and a C-terminal region with undefined function. The PX domain of SNX17 is not required for SNX17 binding to the APP cytoplasmic tail. GST or GST-APP was incubated with lysates from U87 cells stably expressing full-length SNX17 or ΔPX-SNX17 and subjected to Western blotting with anti-Myc antibody. GST-APP, but not GST, binds to both full-length SNX17 and ΔPX-SNX17. *TM*, transmembrane domain.

RESULTS

SNX17 Binds to the APP Cytoplasmic Domain through the YXNPXY Motif—The APP cytoplasmic domain contains a YXNPXY motif that is responsible for binding to several cell surface adaptor proteins (Fig. 1*A*). Because SNX17 binds to LRP1 through an analogous NPXY motif (17), we tested the ability of SNX17 to bind the APP cytoplasmic domain. GST or the GST-fused APP cytoplasmic domain was incubated with lysates from U87 cells stably expressing Myc-tagged SNX17, and binding was examined by Western blotting using anti-Myc antibody. As shown in Fig. 1*A*, the GST-APP tail, but not GST, was able to bind to SNX17 (Fig. 1*A*), suggesting that SNX17 is a novel binding protein for APP. To analyze whether the YXNPXY motif within the APP tail is responsible for SNX17 binding, we mutated each residue within this motif to alanine, and their binding to SNX17 was examined by GST pulldown assay (Fig. 1*A*). We found that mutations of the critical residue Tyr^{757}, Asn^{759}, Pro^{760}, or Tyr^{762} within the YXNPXY motif of the APP tail abrogated its binding to SNX17, indicating that this motif is critical for this interaction. To determine whether the PX domain of SNX17, which is required for the endosomal localization of SNX17, participates in binding to APP, the GST-APP tail was incubated with lysates from U87 cells stably expressing Myc-tagged full-length or PX domain-deleted SNX17, and binding was examined as described above. As shown in Fig. 1*B*, deletion of the PX domain did not affect the

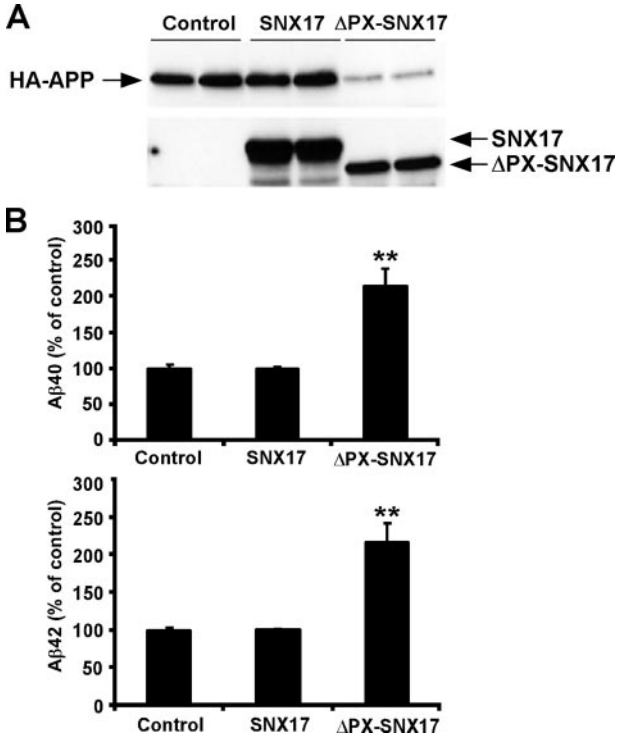

FIGURE 2. **The dominant-negative mutant of SNX17 reduces steady-state levels of APP and increases Aβ production.** *A*, ΔPX-SNX17 decreases cellular APP levels. HA-APP was cotransfected with full-length SNX17 or ΔPX-SNX17, and cellular APP levels were examined by Western blotting using anti-HA antibody. Expressions of SNX17 and ΔPX-SNX17 were confirmed by Western blotting using anti-Myc antibody. *B*, ΔPX-SNX17 increases Aβ production. HA-APP was cotransfected with full-length SNX17 or ΔPX-SNX17, and Aβ40 and Aβ42 levels in the conditioned medium were analyzed by ELISA. The Aβ levels were normalized by expression of green fluorescent protein, cotransfected with APP and SNX17 (not shown). **, $p < 0.01$ compared with the controls.

interaction between SNX17 and the APP cytoplasmic tail, indicating that the PX domain is not required for SNX17 binding to APP. This result is consistent with the previous finding that the SNX17 PX domain is not necessary for the interaction between SNX17 and LRP1 (17) and suggests that the binding domain for APP resides within the carboxyl-terminal domain of SNX17.

SNX17 Regulates APP Processing and Aβ Production—We have shown previously that SNX17 binds to LRP1 through a similar NP*X*Y motif and promotes LRP1 recycling (17). Thus, we reasoned that SNX17 may play an important role in APP endocytic trafficking and processing to Aβ. It has been shown that deletion of the PX domain abrogates the early endosomal localization of SNX17 (15, 23), which is required for its function. Therefore, we analyzed the effects of overexpressing a dominant-negative mutant of SNX17 lacking its PX domain on APP stability and processing. Full-length or PX-deleted SNX17 (indicated as SNX17 or ΔPX-SNX17, respectively, in Fig. 2*A*) was cotransfected with HA-APP into U87 cells, and cellular levels of APP and Aβ production were examined by Western blotting and ELISA, respectively. Coexpression of ΔPX-SNX17 dramatically decreased the steady-state levels of APP compared with full-length SNX17- or pcDNA3 vector-transfected cells (Fig. 2*B*), whereas more Aβ was produced in ΔPX-SNX17-cotransfected cells (Fig. 2*C*).

To further examine SNX17 function in APP processing and Aβ production with an alternative approach, we analyzed cellular APP and secreted Aβ levels in SNX17 knockdown cells. HA-APP and control or SNX17 siRNA oligonucleotide (17) were cotransfected into U87 cells, and the levels of cellular APP and Aβ production were examined by Western blotting and ELISA, respectively. When SNX17 expression was suppressed by siRNA oligonucleotide, cellular levels of APP were greatly reduced compared with control siRNA oligonucleotide-transfected cells (Fig. 3*A*). Quantification of the Western blots from multiple experiments showed that cellular levels of APP were decreased by ~75% when the expression of SNX17 was knocked down by ~90%. To confirm the effect of SNX17 on the decreased cellular levels of APP, SNX17 expression was rescued by cotransfecting cells with an siRNA-resistant SNX17 construct. APP expression was significantly restored when the siRNA-resistant SNX17 construct was cotransfected with SNX17 siRNA oligonucleotide (Fig. 3*B*). We also found that the levels of APP C-terminal fragment were decreased when cells were cotransfected with the siRNA-resistant SNX17 construct (data not shown), suggesting that the APP processing was ameliorated by restoring the expression of SNX17. We also found that cell surface levels of APP were significantly reduced in SNX17 knockdown cells compared to control siRNA oligonucleotide-treated cells (data not shown), consistent with the previous report that knockdown of SNX17 expression decreases the cell surface levels of LRP (17). Reduced cellular levels of APP in SNX17 knockdown cells may be due to a faster turnover of APP when SNX17 expression is knocked down. Thus, the half-life of APP was examined in SNX17 knockdown cells and control siRNA oligonucleotide-treated cells using cycloheximide to inhibit new protein synthesis. Consistent with our hypothesis, the half-life of APP was significantly reduced in SNX17 knockdown cells ($t_{1/2}$ ~ 42 min) compared to control siRNA oligonucleotide-treated cells ($t_{1/2}$ ~ 98 min) (Fig. 3*C*). Results from metabolic pulse-chase experiments using [^{35}S]Met/Cys also showed that the half-life of APP was greatly reduced in SNX17 knockdown cells ($t_{1/2}$ ~ 21 min) compared to control siRNA-treated cells ($t_{1/2}$ ~ 43 min) (Fig. 3*D*). We also found that Aβ production was increased in SNX17 knockdown cells (Fig. 3*E*), consistent with the results using dominant-negative ΔPX-SNX17. Together, these data suggest that SNX17 function is critical for the cell surface localization and stability of APP. When SNX17 function is reduced, APP is more likely to undergo amyloidogenic processing.

SNX17 Colocalizes with APP and Is Highly Expressed in Central Nervous System Neurons—APP is a type I transmembrane protein that is internalized and traffics through the endocytic pathway. SNX17 is localized to the early endosome (17). To examine whether APP is present in SNX17-containing endosomes, U87 cells transiently transfected with HA-APP were incubated with anti-HA antibody for 1 h at 37 °C, fixed, and then stained with anti-SNX17 antibody, followed by detection with secondary antibodies. Because the HA tag is at the N terminus of APP, anti-HA antibody uptake represents the APP that has been internalized from the cell surface without contribution from the population in the biosynthetic pathway. Fig. 4*C* shows that SNX17 and APP are partially colocalized in punctate perinuclear structures. To identify the subcellular compartments containing APP, U87 cells were stained for the early

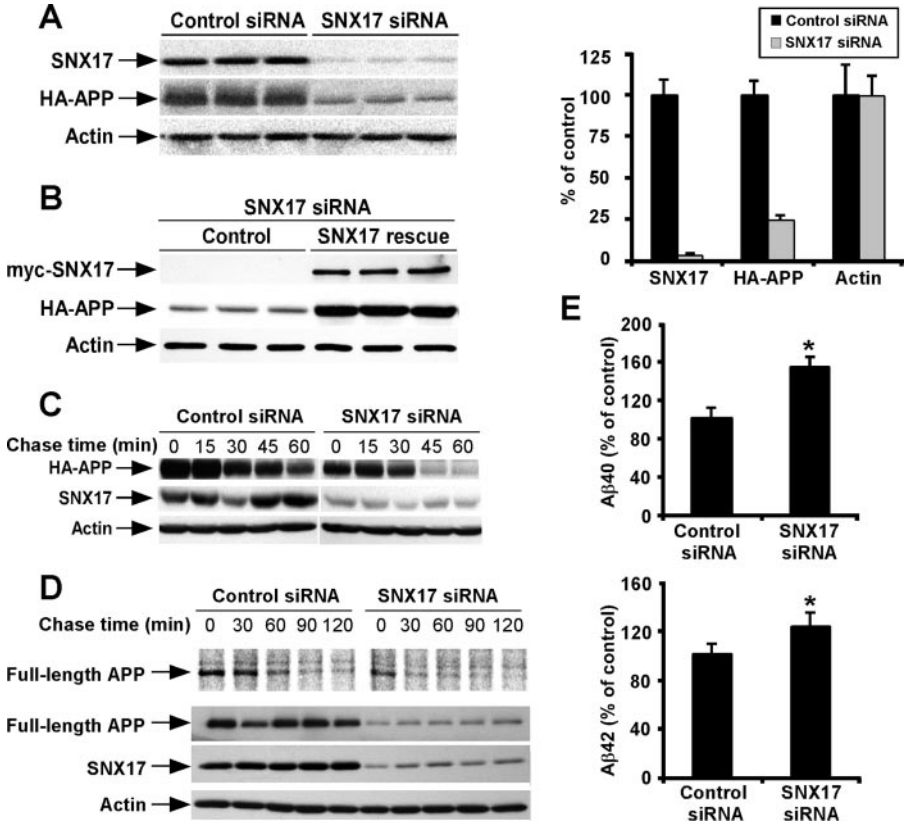

FIGURE 3. **SNX17 regulates APP cell surface levels, turnover, and Aβ production.** *A*, SNX17 knockdown decreases cellular APP levels. Control or SNX17 siRNA oligonucleotides were cotransfected with HA-APP into U87 cells, and the levels of APP were examined by Western blotting with anti-HA antibody. Quantification of SNX17, APP, and actin Western blots is shown in the *right panel*. *B*, the cellular level of APP was restored when an siRNA oligonucleotide-resistant SNX17 construct was cotransfected with SNX17 siRNA. Western blot analysis was performed using U87 cells cotransfected with HA-APP, SNX17 siRNA, and either control vector or siRNA-resistant SNX17 construct. *C*, SNX17 knockdown decreases APP half-life. U87 cells were cotransfected with HA-APP and either control or SNX17 siRNA. After 48 h, cells were incubated with cycloheximide for 0, 15, 30, 45, or 60 min, followed by Western blotting with anti-HA antibody. *D*, SNX17 knockdown decreases APP half-life, detected by pulse-chase analysis. U87 cells were cotransfected with HA-APP and either control or SNX17 siRNA. After 48 h, cells were incubated with medium containing [^{35}S]Met/Cys for 30 min and chased with medium without [^{35}S]Met/Cys for 0, 30, 60, or 120 min, followed by immunoprecipitation with anti-HA antibody. Radiolabeled APP bands were visualized after SDS-PAGE. *E*, SNX17 knockdown increases Aβ production. Aβ40 and Aβ42 levels in the conditioned medium from U87 cells cotransfected with HA-APP and either control or SNX17 siRNA were analyzed by ELISA. *, $p < 0.05$ compared with the controls.

endosomal marker, EEA1, after anti-HA antibody uptake. As shown in Fig. 4, *D–F*, APP also partially colocalized with EEA1. Because SNX17 and EEA1 are localized in the same endosomal compartments (Fig. 4, *G–I*), these results indicate that cell surface APP enters early endosomes after internalization and likely interacts with SNX17 in these compartments.

It has been shown that SNX17 mRNA is highly expressed in brain and liver (24); however, SNX17 expression has not been analyzed at the protein level. We examined SNX17 expression in mouse brain tissues by Western blotting using anti-SNX17 antibody. Significant amounts of SNX17 were detected in different regions of the brain where LRP1 and APP are also expressed. To determine whether SNX17 is expressed in neurons of the brain, Western blot analysis was performed using primary cultured cortical and hippocampal neurons. As shown in Fig. 5*B*, SNX17, as well as LRP1 and APP, is expressed in both types of neurons. To examine whether SNX17 and APP are colocalized in neurons, primary cultured hippocampal neurons were stained for endogenous SNX17 and APP. Consistent with the results from U87 cells, SNX17 and APP are highly colocalized in hippocampal neurons, including punctate structures within their processes (*arrows* in Fig. 5*C*).

Dab2 Binds to APP and Regulates APP Endocytosis—Dab2 binds to the NP*X*Y motifs of LDLR and ApoER2 and mediates their endocytosis through clathrin-coated pits (8, 25, 26). Dab2 contains a PTB domain, which interacts with both target proteins and the phosphoinositide moieties of certain lipids (27). It has been shown that Dab2 binds to an NP*X*Y motif-containing peptide corresponding to a portion of the APP cytoplasmic domain; however, whether Dab2 serves as an endocytic adaptor for APP is not known. First, we confirmed by GST pulldown assay that Dab2 binds directly to APP. GST-Dab2 proteins were incubated with lysates from cells expressing wild-type HA-APP or NP*X*Y mutants, and binding was detected by Western blotting with anti-HA antibody. Consistent with a previous report (8), Dab2 binds to the NP*X*Y motif of APP (Fig. 6*A*). In parallel experiments, binding between Dab2 and ApoER2 was also confirmed as a positive control (data not shown). Binding of APP to the GST-Dab2 PTB domain was stronger than that to GST-full-length Dab2. Next, we asked whether Dab2 affects the cell surface level and internalization of APP. The Dab2 PTB domain has been shown to act as a dominant-negative mutant of Dab2, as overexpression of this construct inhibits the endocytosis of LDLR (25). To determine whether Dab2 affects APP endocytosis, Dab2 and HA-APP were cotransfected into CHO LRP-null cells, and APP internalization was assessed. As shown in Fig. 6*B*, Dab2 overexpression increased, whereas PTB domain overexpression decreased, the internalization of APP, similar to the effect that the Dab2 PTB domain has on the endocytosis of LDLR and ApoER2 (25, 26). This suggests that Dab2 serves as an endocytic adaptor protein for APP. Consistently, overexpression of the Dab2 PTB domain increased the cell surface levels of APP (Fig. 6*C*), suggesting that the dominant-negative function of the PTB domain blocked the normal function of Dab2 in facilitating APP internalization. Aβ levels from U87 cells transiently transfected with HA-APP and full-length Dab2 or the Dab2 PTB domain were analyzed by ELISA. Interestingly, overexpression of full-length Dab2 increased, whereas the Dab2 PTB domain decreased, Aβ

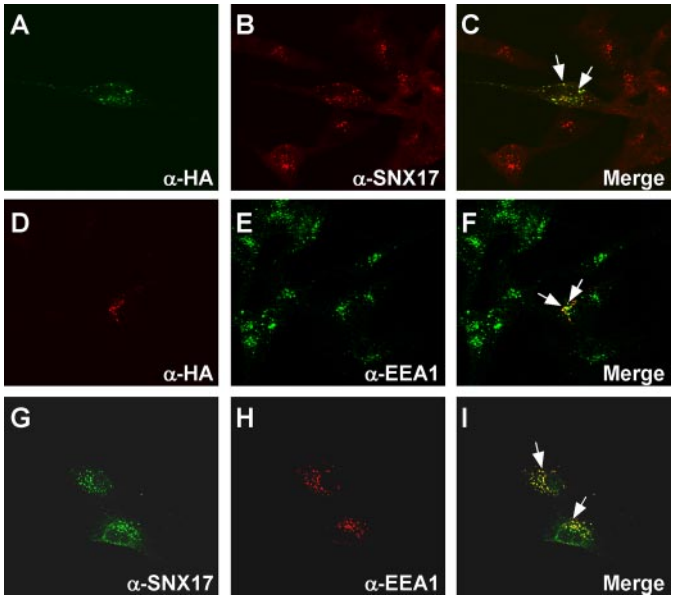

FIGURE 4. **APP and SNX17 colocalize in the early endosomes.** U87 cells transiently transfected with HA-APP were incubated with anti-HA IgG at 37 °C for 1 h, fixed, and then stained with anti-SNX17 (*A* and *B*) or anti-EEA1 (*D* and *E*), followed by secondary antibodies. APP is found in both SNX17- and EEA1-positive compartments (*C* and *F*). SNX17 and EEA1 are highly colocalized (*G–I*). *Arrows* highlight staining with significant colocalization.

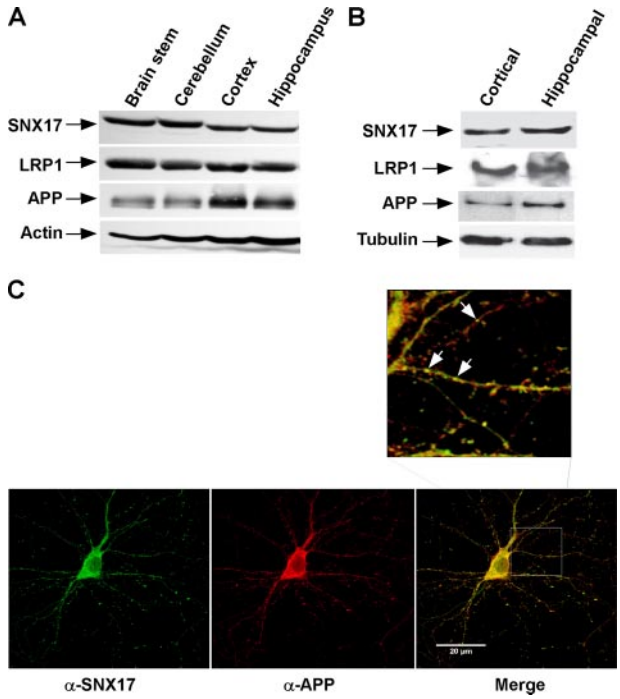

FIGURE 5. **SNX17 is highly expressed in mouse brain and colocalizes with APP in primary neurons.** *A*, SNX17 is highly expressed in several regions of adult mouse brain where APP and LRP1 are also highly expressed. *B*, SNX17 is highly expressed in primary cultured cortical and hippocampal neurons. *C*, SNX17 and APP are colocalized in primary hippocampal neurons. Primary hippocampal neurons were co-stained with anti-SNX17 and anti-APP antibodies. A region including several neuronal processes is shown in higher magnifications. *Arrows* highlight staining with significant colocalization.

production (Fig. 6*D*). Overall, these results suggest that Dab2 facilitates APP endocytosis, which in turn favors the amyloidogenic processing of APP.

DISCUSSION

In this study, we defined the functions of two intracellular adaptor proteins, SNX17 and Dab2, in regulating APP trafficking and processing to Aβ in distinct cellular compartments. Aβ is generated from APP by proteolytic processing, and its aggregation is toxic to neurons. The rate of Aβ production is considered to be a major determining factor in the onset of AD (1, 2, 28). Several studies on APP trafficking have shown that the subcellular localization of APP greatly affects the rate of Aβ production. Newly synthesized APP molecules are largely cleaved into soluble APPα by α-secretase at the cell surface (non-amyloidogenic pathway); however, APP molecules that are internalized from the plasma membrane are delivered to the endocytic compartments, where they are processed by β-secretase and subsequently by γ-secretase into soluble APPβ and Aβ (amyloidogenic pathway). Because the amyloidogenic pathway is favored when APP is internalized into endosomal compartments, promoting the recycling of APP to the cell surface may be one way to reduce Aβ production (1, 3).

There are several cell surface adaptor proteins, including Fe65 and X11, shown to bind to APP and affect APP internalization and processing to Aβ. For example, Fe65 increases, whereas X11 decreases, Aβ secretion by regulating the cell surface levels of APP (6, 7, 9, 10, 29). In this report, we characterized the function of Dab2 in APP trafficking and processing to Aβ. Dab2 has been known as an adaptor protein for the endocytosis of several LDLR family members, including LDLR, megalin, and ApoER2, by binding to the NP*X*Y motifs in their cytoplasmic domains (8, 25, 26, 30, 31) while simultaneously binding to clathrin and other clathrin adaptors. Although it has been shown that Dab2 binds to a 15-amino acid-long synthetic peptide containing the NP*X*Y motif of APP *in vitro* (8), its function in APP trafficking remained unstudied. First, we confirmed by GST pulldown assays that Dab2 binds to the APP cytoplasmic domain through the NP*X*Y motif (Fig. 6*A*). We observed that overexpression of full-length Dab2 increases, whereas the dominant-negative Dab2 PTB domain decreases, the internalization of APP, which is consistent with previous studies on the effects of Dab2 on LDLR family members (25). As expected, overexpression of the Dab2 PTB domain increased the cell surface level of APP, which resulted in decreased Aβ production, whereas full-length Dab2 had the opposite effect (Fig. 6*D*). These results are consistent with previous reports showing that the regulation of cell surface levels of APP alters Aβ production.

In addition to cell surface adaptor proteins, increasing numbers of APP-binding proteins, mostly transmembrane proteins, including several LDLR family members, have been identified and shown to affect APP trafficking and processing to Aβ (7, 29). LRP1 binds to APP and facilitates APP internalization, which results in increased Aβ production (4), whereas LRP1B, a homologue of LRP1 with a slow endocytosis rate, inhibits APP internalization and reduces Aβ production (32). ApoER2 also increases APP processing to Aβ by recruiting APP into lipid rafts and increasing γ-secretase activity (33). In addition, SorLA, another member of the LDLR family mainly localized to the Golgi, binds to APP and is thought to mediate its transport from endosomes to the Golgi, where less Aβ is produced (5, 34,

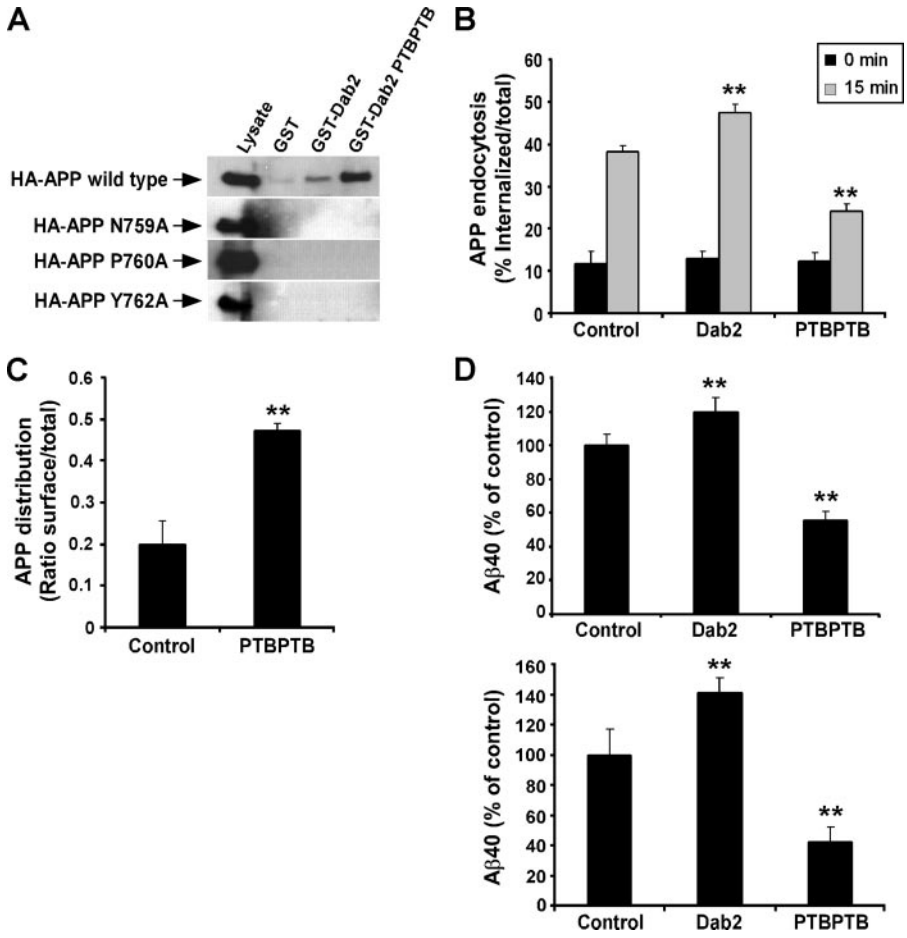

FIGURE 6. **Dab2 mediates APP endocytosis.** *A*, Dab2 directly interacts with APP through the NP*X*Y motif. GST, GST-Dab2, or GST-Dab2 PTBPTB (tandem PTB) was incubated with lysates from CHO LRP-null cells transiently transfected with wild-type HA-APP or mutants and subjected to Western blotting with anti-HA antibody. GST-Dab2 protein binds to wild-type APP but not to NP*X*Y mutants. Stronger binding to APP was detected with the tandem PTB domain construct compared with full-length Dab2. *B*, Dab2 facilitates APP endocytosis. Endocytosis of APP, measured 15 min after 37 °C incubation, is increased in Dab2-transfected cells and decreased in the dominant-negative mutant-containing PTB domain-transfected cells. *C*, the cell surface levels of APP are increased in cells transfected with the PTB domain. CHO LRP-null cells stably transfected with control vector or the Dab2 PTBPTB domain were analyzed for the ratios of cell surface and total APP. *D*, full-length Dab2 increases, whereas the Dab2 PTB domain decreases, Aβ production. Aβ40 and Aβ42 levels in the conditioned medium from U87 cells cotransfected with HA-APP and pcDNA3, full-length Dab2, or the Dab2 PTB domain were analyzed by ELISA. **, $p < 0.01$ compared with the controls.

35). Because Aβ production is greatly affected by the subcellular localization of APP, it is important to identify regulators of the subcellular localization and trafficking of APP. However, there are currently no reports showing that cytoplasmic proteins localized to specific intracellular compartments, such as endosomes, bind to APP and regulate APP trafficking and processing to Aβ.

Here, for the first time we identify SNX17 as an intracellular adaptor protein for APP. SNX17 binds directly to the Y*X*NP*X*Y motif in the APP cytoplasmic domain (Fig. 1*A*). Although many sorting nexins are known to participate in intracellular protein trafficking, SNX17 is unique because it is the only sorting nexin known to recognize a specific signal in the cytoplasmic domain of target proteins. It recognizes the NP*X*Y motif of several members of the LDLR family and regulates their endocytic trafficking (15, 17). By recognizing the same motif in the APP cytoplasmic domain, NP*X*Y, SNX17 regulates the intracellular trafficking of APP and affects Aβ production. Our work has shown previously that SNX17 promotes LRP1 recycling by binding to the NP*X*Y motif of LRP1 (17). The cell surface levels of LRP1 are decreased in SNX17 knockdown cells compared to control cells; accordingly, its ability to degrade ligands was decreased. In addition, the degradation of LRP1 was facilitated when its binding to SNX17 was impaired. Consistent with this, the steady-state levels of cellular APP are decreased in SNX17 knockdown cells, caused by a faster turnover of APP, presumably due to inefficient recycling of APP (Fig. 3, *A* and *C*). APP has been shown to be recycled efficiently after internalization, but the mechanism by which this recycling occurs has not been studied (36, 37). Because of the relatively low expression level and short half-life of endogenous APP, we performed the majority of our work with overexpressed APP, a strategy commonly used for studying APP trafficking and processing. We propose that SNX17 mediates APP recycling to the cell surface by direct interaction through the NP*X*Y motif in the APP cytoplasmic domain. We found that the cell surface levels of APP were decreased in SNX17 knockdown cells compared to the control cells (data not shown), although the difference was small. The small difference detected here could be due to the fast and serial processing of APP, which might interfere with the quantification. It is interesting to note that knockdown of SNX17 decreases the steady-state level of APP, accompanied with an increase in Aβ production. This suggests that β-cleavage of APP partially but significantly contributes to the faster turnover of APP when SNX17 is knocked down. The PX domain of SNX17 is required for its endosomal localization but not for its binding to target proteins (15, 17). Although deletion of the PX domain of SNX17 did not disrupt SNX17 binding to APP (Fig. 1*B*), it greatly reduced the level of cellular APP and increased Aβ production, suggesting that the endosomal localization of SNX17 is required for its proper function in APP trafficking (Fig. 2). Although potential alterations of SNX17 expression in the AD brains remain to be studied, our results indicate that facilitating APP interaction with SNX17 might be a possible strategy for reducing Aβ production in AD.

It is interesting that the same motif in the APP cytoplasmic domain, Y*X*NP*X*Y, binds to a growing number of cytoplasmic adaptor proteins. Depending on the subcellular localization,

APP binds to different adaptor proteins, and these interactions affect APP trafficking, turnover, and processing to Aβ. It is attractive to speculate that several of these adaptor proteins, such as Fe65, X11, Dab1, and Dab2, compete with one another for binding to APP at the cell surface and that their dominance in APP binding is likely influenced by their relative expression levels and affinity for APP. To our knowledge, SNX17 is the only adaptor protein that is localized in endosomal compartments that bind to the Y*X*NP*X*Y motif of APP. The recognition pattern and regulation of APP trafficking by the cell surface adaptor protein, Dab2, and the intracellular adaptor protein, SNX17, closely resemble those of LDLR.

Recently it was found that the expression of SorLA is decreased in AD brains (5, 34, 38) and that inherited variants in the SorLA gene, *SORL1*, are associated with late-onset AD (38). Although we showed that SNX17 is expressed in neurons where APP is also expressed, it is not known whether the expression and function of SNX17 and Dab2 are altered in AD brains. In this regard, it will be interesting to investigate whether the expression levels of SNX17 and Dab2 change during aging and/or AD. Understanding the functions of APP-interacting proteins may allow us to identify specific drug targets for AD therapy.

Acknowledgments—We thank Johannes Nimpf, Thomas C. Südhof, Kelly Bales, and Steven Paul (Lilly Research Laboratories) and Linton Traub for providing valuable reagents for this research. We also thank Jane Knisely, Stuart Kornfeld, Maurine Linder, Jonathan Gitlin, David Harris, and Mike Mueckler for critical reading of this manuscript and Pamela Farfan and Claudia Araya for technical support in the fluorescence-activated cell sorter experiments.

REFERENCES

1. Selkoe, D. J. (2001) *Physiol. Rev.* **81,** 741–766
2. Zheng, H., and Koo, E. H. (2006) *Mol. Neurodegener.* **1,** 5
3. Cam, J. A., and Bu, G. (2006) *Mol. Neurodegener.* **1,** 8
4. Cam, J. A., Zerbinatti, C. V., Li, Y., and Bu, G. (2005) *J. Biol. Chem.* **280,** 15464–15470
5. Andersen, O. M., Reiche, J., Schmidt, V., Gotthardt, M., Spoelgen, R., Behlke, J., von Arnim, C. A., Breiderhoff, T., Jansen, P., Wu, X., Bales, K. R., Cappai, R., Masters, C. L., Gliemann, J., Mufson, E. J., Hyman, B. T., Paul, S. M., Nykjaer, A., and Willnow, T. E. (2005) *Proc. Natl. Acad. Sci. U. S. A.* **102,** 13461–13466
6. Miller, C. C., McLoughlin, D. M., Lau, K. F., Tennant, M. E., and Rogelj, B. (2006) *Trends Neurosci.* **29,** 280–285
7. Borg, J. P., Ooi, J., Levy, E., and Margolis, B. (1996) *Mol. Cell. Biol.* **16,** 6229–6241
8. Morris, S. M., and Cooper, J. A. (2001) *Traffic* **2,** 111–123
9. Sabo, S. L., Lanier, L. M., Ikin, A. F., Khorkova, O., Sahasrabudhe, S., Greengard, P., and Buxbaum, J. D. (1999) *J. Biol. Chem.* **274,** 7952–7957
10. Xie, Z., Dong, Y., Maeda, U., Xia, W., and Tanzi, R. E. (2007) *J. Biol. Chem.* **282,** 4318–4325
11. Hoe, H. S., Tran, T. S., Matsuoka, Y., Howell, B. W., and Rebeck, G. W. (2006) *J. Biol. Chem.* **281,** 35176–35185
12. Haft, C. R., de la Luz Sierra, M., Barr, V. A., Haft, D. H., and Taylor, S. I. (1998) *Mol. Cell. Biol.* **18,** 7278–7287
13. Seet, L. F., and Hong, W. (2006) *Biochim. Biophys. Acta* **1761,** 878–896
14. Worby, C. A., and Dixon, J. E. (2002) *Nat. Rev. Mol. Cell Biol.* **3,** 919–931
15. Burden, J. J., Sun, X. M., Garcia, A. B., and Soutar, A. K. (2004) *J. Biol. Chem.* **279,** 16237–16245
16. Stockinger, W., Sailler, B., Strasser, V., Recheis, B., Fasching, D., Kahr, L., Schneider, W. J., and Nimpf, J. (2002) *EMBO J.* **21,** 4259–4267
17. van Kerkhof, P., Lee, J., McCormick, L., Tetrault, E., Lu, W., Schoenfish, M., Oorschot, V., Strous, G. J., Klumperman, J., and Bu, G. (2005) *EMBO J.* **24,** 2851–2861
18. Li, Y., Marzolo, M. P., van Kerkhof, P., Strous, G. J., and Bu, G. (2000) *J. Biol. Chem.* **275,** 17187–17194
19. Bu, G., Maksymovitch, E. A., Geuze, H., and Schwartz, A. L. (1994) *J. Biol. Chem.* **269,** 29874–29882
20. Bu, G., Geuze, H. J., Strous, G. J., and Schwartz, A. L. (1995) *EMBO J.* **14,** 2269–2280
21. Johnson-Wood, K., Lee, M., Motter, R., Hu, K., Gordon, G., Barbour, R., Khan, K., Gordon, M., Tan, H., Games, D., Lieberburg, I., Schenk, D., Seubert, P., and McConlogue, L. (1997) *Proc. Natl. Acad. Sci. U. S. A.* **94,** 1550–1555
22. Melman, L., Geuze, H. J., Li, Y., McCormick, L. M., Van Kerkhof, P., Strous, G. J., Schwartz, A. L., and Bu, G. (2002) *Mol. Biol. Cell* **13,** 3325–3335
23. Williams, R., Schluter, T., Roberts, M. S., Knauth, P., Bohnensack, R., and Cutler, D. F. (2004) *Mol. Biol. Cell* **15,** 3095–3105
24. Florian, V., Schluter, T., and Bohnensack, R. (2001) *Biochem. Biophys. Res. Commun.* **281,** 1045–1050
25. Mishra, S. K., Keyel, P. A., Hawryluk, M. J., Agostinelli, N. R., Watkins, S. C., and Traub, L. M. (2002) *EMBO J.* **21,** 4915–4926
26. Cuitino, L., Matute, R., Retamal, C., Bu, G., Inestrosa, N. C., and Marzolo, M. P. (2005) *Traffic* **6,** 820–838
27. Yun, M., Keshvara, L., Park, C. G., Zhang, Y. M., Dickerson, J. B., Zheng, J., Rock, C. O., Curran, T., and Park, H. W. (2003) *J. Biol. Chem.* **278,** 36572–36581
28. Oltersdorf, T., Fritz, L. C., Schenk, D. B., Lieberburg, I., Johnson-Wood, K. L., Beattie, E. C., Ward, P. J., Blacher, R. W., Dovey, H. F., and Sinha, S. (1989) *Nature* **341,** 144–147
29. Zambrano, N., Buxbaum, J. D., Minopoli, G., Fiore, F., De Candia, P., De Renzis, S., Faraonio, R., Sabo, S., Cheetham, J., Sudol, M., and Russo, T. (1997) *J. Biol. Chem.* **272,** 6399–6405
30. Maurer, M. E., and Cooper, J. A. (2006) *J. Cell Sci.* **119,** 4235–4246
31. Gallagher, H., Oleinikov, A. V., Fenske, C., and Newman, D. J. (2004) *Biochimie* (*Paris*) **86,** 179–182
32. Cam, J. A., Zerbinatti, C. V., Knisely, J. M., Hecimovic, S., Li, Y., and Bu, G. (2004) *J. Biol. Chem.* **279,** 29639–29646
33. Fuentealba, R. A., Barria, M., Lee, J., Cam, J., Araya, C., Escudero, C. A., Inestrosa, N. C., Bronfman, F. C., Bu, G., and Marzolo, M. P. (2007) *Mol. Neurodegener.* **2,** 14
34. Andersen, O. M., Schmidt, V., Spoelgen, R., Gliemann, J., Behlke, J., Galatis, D., McKinstry, W. J., Parker, M. W., Masters, C. L., Hyman, B. T., Cappai, R., and Willnow, T. E. (2006) *Biochemistry* **45,** 2618–2628
35. Shah, S., and Yu, G. (2006) *Mol. Interv.* **6,** 74–76
36. Yamazaki, T., Koo, E. H., and Selkoe, D. J. (1996) *J. Cell Sci.* **109,** 999–1008
37. Koo, E. H., Squazzo, S. L., Selkoe, D. J., and Koo, C. H. (1996) *J. Cell Sci.* **109,** 991–998
38. Rogaeva, E., Meng, Y., Lee, J. H., Gu, Y., Kawarai, T., Zou, F., Katayama, T., Baldwin, C. T., Cheng, R., Hasegawa, H., Chen, F., Shibata, N., Lunetta, K. L., Pardossi-Piquard, R., Bohm, C., Wakutani, Y., Cupples, L. A., Cuenco, K. T., Green, R. C., Pinessi, L., Rainero, I., Sorbi, S., Bruni, A., Duara, R., Friedland, R. P., Inzelberg, R., Hampe, W., Bujo, H., Song, Y. Q., Andersen, O. M., Willnow, T. E., Graff-Radford, N., Petersen, R. C., Dickson, D., Der, S. D., Fraser, P. E., Schmitt-Ulms, G., Younkin, S., Mayeux, R., Farrer, L. A., and St George-Hyslop, P. (2007) *Nat. Genet.* **39,** 168–177